

# GPS-BASED OPTIMAL KALMAN ESTIMATION OF TIME ERROR, FREQUENCY OFFSET, AND AGING

Yu. S. Shmaliy\*, A. V. Marienko\*\*, and A. V. Savchuk\*\*\*

\*Electronics Dept., Guanajuato University, Salamanca, 36730, Mexico

\*\*St. Co. IRVA, Kiev, Ukraine

\*\*\*Ukrainian Sci. Res. Institute for Communication, Kiev, Ukraine

*mtorres@salamanca.ugto.mx*

## Abstract

*Results are presented of studies of different types of optimal and quasi-optimal Kalman filters based on crystal and rubidium oscillators using reference timing signals from the Motorola GPS UT + Oncore Timing receiver. Filter equations are considered for different definitions of their coefficients, and the filter output signal and its statistics are investigated in time under real conditions. Various Kalman algorithms and corresponding optimal filter structures intended for crystal and rubidium oscillators are discussed. Three-dimensional Kalman filters intended for optimal estimation of time error, frequency offset, and frequency aging are considered based on the oscillator signal model. One application is the synchronization needs of digital communication networks and metrology. Results are given for the measured data and estimates are compared with respect to a quartz crystal oscillator. Practical results are considered of the Kalman filter's use in application to an oven-controlled quartz crystal oscillator (OCXO) with an AT-cut resonator. Plots of the original and filtered processes are discussed for the different approaches to definition of the Kalman filter coefficients. Estimates are also given for the filtering errors and the processing rate.*

## INTRODUCTION

Fast and accurate optimal Kalman filtering of the time error, frequency, and frequency offset of slaved sources (crystal and rubidium) is extremely important to create frequency and time standards looked after GPS timing signals. It is known that excellent accuracy less than  $10^{-12}$  is obtained in practice approximately through 24 hours, based on a smoothing filter. It is the reason why efforts are now underway in direction of the fast Kalman algorithm creation to obtain the same accuracy for the minimal processing time. Allan and Barnes in [1] showed that the filtering effect strongly depends on a measuring time interval  $\Delta$  and that it must be of 100...1000 sec. Later, series of reports have been devoted to the Kalman filters application, especially for phase, time, and frequency real-time estimates with prediction [2-5]. The papers are based on the Kalman fundamental approach [6] for the discrete-time optimal linear signal estimation with a white Gaussian noise and developed later by many authors in [7-8], for instance.

The report addresses to the results of the various discrete-time Kalman algorithms (one-, two-, and three-state) use for the estimation of synchronization errors being based on the timing signals of Motorola Oncore UT+ Receiver. Once the purpose was to compare the various Kalman algorithms, then the results were found for one OCXO unit with an AT-cut resonator. While doing so, we dealt with many measured and estimated functions of the time error, frequency, and aging related to the OCXO and rubidium standard. It allowed comparison and selection of appropriate optimal filter structure separately for each type of an oscillator and for measurement and synchronization tasks. As it was expected, different algorithms gave different filtering errors. Only when the frequency drift showed a quasi-stationary nature did it not matter what type of Kalman filter was used. On the contrary, in the non-stationary case only optimal filtering and control algorithms provide sufficient accuracy. Here the major point is the timing model of the steered source. One must expect that a rubidium source of frequency may be disciplined by GPS signals with relatively small error in comparison with the crystal one, because of good a priori prediction of the phase behavior in time. We study major of these possibilities in the report.

Report Documentation Page				Form Approved OMB No. 0704-0188	
Public reporting burden for the collection of information is estimated to average 1 hour per response, including the time for reviewing instructions, searching existing data sources, gathering and maintaining the data needed, and completing and reviewing the collection of information. Send comments regarding this burden estimate or any other aspect of this collection of information, including suggestions for reducing this burden, to Washington Headquarters Services, Directorate for Information Operations and Reports, 1215 Jefferson Davis Highway, Suite 1204, Arlington VA 22202-4302. Respondents should be aware that notwithstanding any other provision of law, no person shall be subject to a penalty for failing to comply with a collection of information if it does not display a currently valid OMB control number.					
1. REPORT DATE <b>DEC 1999</b>		2. REPORT TYPE		3. DATES COVERED <b>00-00-1999 to 00-00-1999</b>	
4. TITLE AND SUBTITLE <b>GPS-Based Optimal Kalman Estimation of Time Error, Frequency Offset, and Aging</b>				5a. CONTRACT NUMBER	
				5b. GRANT NUMBER	
				5c. PROGRAM ELEMENT NUMBER	
6. AUTHOR(S)				5d. PROJECT NUMBER	
				5e. TASK NUMBER	
				5f. WORK UNIT NUMBER	
7. PERFORMING ORGANIZATION NAME(S) AND ADDRESS(ES) <b>Guanajuato University, Electronics Dept, Salamanca, 36730, Mexico,</b>				8. PERFORMING ORGANIZATION REPORT NUMBER	
9. SPONSORING/MONITORING AGENCY NAME(S) AND ADDRESS(ES)				10. SPONSOR/MONITOR'S ACRONYM(S)	
				11. SPONSOR/MONITOR'S REPORT NUMBER(S)	
12. DISTRIBUTION/AVAILABILITY STATEMENT <b>Approved for public release; distribution unlimited</b>					
13. SUPPLEMENTARY NOTES <b>See also ADM001481. 31st Annual Precise Time and Time Interval (PTTI) Planning Meeting, 7-9 December 1999, Dana Point, CA</b>					
14. ABSTRACT <b>see report</b>					
15. SUBJECT TERMS					
16. SECURITY CLASSIFICATION OF:			17. LIMITATION OF ABSTRACT <b>Same as Report (SAR)</b>	18. NUMBER OF PAGES <b>10</b>	19a. NAME OF RESPONSIBLE PERSON
a. REPORT <b>unclassified</b>	b. ABSTRACT <b>unclassified</b>	c. THIS PAGE <b>unclassified</b>			

## DISCRETE-TIME KALMAN FILTER MODEL

The oscillator or clock discrete-time equations are given by observation and state vectors [9]

$$\xi_v = \mathbf{H}_v \lambda_v + \mathbf{u}_v + \mathbf{n}_{0v}, \quad (1)$$

$$\lambda_v = \mathbf{A}_{v-1} \lambda_{v-1} + \mathbf{n}_{\lambda v}, \quad (2)$$

where  $v = 0, 1, 2, \dots$  corresponds to discrete-time  $t_v$  and measuring time interval  $\Delta = t_v - t_{v-1}$ ,  $\xi_v = \xi(t_v)$  is  $m$ -dimensional observation vector formed by the reference short-term noisy GPS timing signals and the oscillator,  $\lambda_v = \lambda(t_v)$  is  $n$ -dimensional oscillator state vector (time, phase, frequency, aging, ...),  $\mathbf{H}_v = \mathbf{H}(t_v)$  is  $m \times n$  dimensional measurement matrix,  $\mathbf{u}_v = \mathbf{u}(t_v)$  is  $m$ -dimensional vector contains the control signals,  $\mathbf{A}_v = \mathbf{A}(t_v)$  is  $n \times n$  dimensional state transition matrix,  $\mathbf{n}_{0v} = \mathbf{n}_0(t_v)$  and  $\mathbf{n}_{\lambda v} = \mathbf{n}_\lambda(t_v)$  are jointly independent vector white noises with zero expectations and covariance matrixes  $\mathbf{V}_v = \mathbf{V}(t_v)$  and  $\Psi_v = \Psi(t_v)$  are of  $m \times m$  and  $n \times n$  dimensions correspondingly

$$\mathbf{V}_v = E\{\mathbf{n}_{0v} \mathbf{n}_{0v}^T\}, \quad (3)$$

$$\Psi_v = E\{\mathbf{n}_{\lambda v} \mathbf{n}_{\lambda v}^T\}. \quad (4)$$

As usual, they deal with single observations and estimate some states of an oscillator or clock. It means, by expansion that if  $m < n$  then one may use the following algorithm of linear Kalman filtering based on (1) and (2)

$$\hat{\lambda}_v = \mathbf{A}_{v-1} \hat{\lambda}_{v-1} + \mathbf{K}_v (\xi_v - \mathbf{u}_v - \mathbf{H}_v \mathbf{A}_{v-1} \hat{\lambda}_{v-1}), \quad (5)$$

$$\mathbf{R}_v = (\mathbf{I} - \mathbf{K}_v \mathbf{H}_v) \tilde{\mathbf{R}}_v, \quad (6)$$

$$\tilde{\mathbf{R}}_v = \mathbf{A}_{v-1} \mathbf{R}_{v-1} \mathbf{A}_{v-1}^T + \Psi_v, \quad (7)$$

$$\mathbf{K}_v = \tilde{\mathbf{R}}_v \mathbf{H}_v^T (\mathbf{H}_v \tilde{\mathbf{R}}_v \mathbf{H}_v^T + \mathbf{V}_v)^{-1}, \quad (8)$$

where  $\hat{\lambda}_v = \lambda(t_v)$  is a vector of oscillator state estimates,  $\mathbf{I}$  is unit matrix, and  $\mathbf{R}_v = \mathbf{R}(t_v)$  is the error covariance matrix. Solution (5) is justified for a common case and may not be simplified, as a rule. Nevertheless, in simple particular cases, one-dimensional algorithms may be sufficient. Setting  $n = m = 1$  in (5)–(8) we come to the following general form for the estimate

$$\hat{\lambda}_v = \beta_{v-1} \hat{\lambda}_{v-1} + k_v (\xi_v - u_v - H_v \beta_{v-1} \hat{\lambda}_{v-1}), \quad (9)$$

$$\frac{1}{R_v} = \frac{1}{\beta_{v-1}^2 R_{v-1} + D_{\lambda v}} + \frac{H_v^2}{D_{0v}}, \quad (10)$$

$$k_v = H_v \frac{R_v}{D_{0v}}, \quad (11)$$

where all the denotes correspond to the vector case.

## ONE-DIMENSIONAL ESTIMATES

Based on (5)–(8) we consider below some particular algorithms of one-dimensional Kalman filters intended for frequency estimation only in crystal and rubidium oscillators if GPS timing signals are used as the reference ones. All results given are obtained with the Motorola Oncore UT+ Receiver.

### STATIONARY KALMAN FILTER

Let  $\beta_v = \beta$ ,  $D_{\lambda v} = D_\lambda$ ,  $H_v = H$ ,  $u_v = u$ , and  $D_{0v} = D_0$  be the constant values in time and the limit  $R_{st} = \lim_{v \rightarrow \infty} R_v$  be known. In this case, the following equation forms the Kalman estimate

$$\hat{\lambda}_v = \beta \hat{\lambda}_{v-1} + H \frac{R_{st}}{D_0} (\xi_v - u_v - H \beta \hat{\lambda}_{v-1}), \quad (12)$$

which is the stationary and non-optimal one, strictly speaking. Taking, as usual, that  $H = 1$ ,  $\beta = 1$ , and  $u = 0$  we transfer to the most simple form of the stationary Kalman filter

$$\hat{\lambda}_v = \hat{\lambda}_{v-1} + \frac{R_{st}}{D_0} (\xi_v - \hat{\lambda}_{v-1}), \quad (13)$$

where  $R_{st}$  is defined from (10) with  $t \rightarrow \infty$  and  $R_v = R_{v-1}$  by the equation  $R_v^2 + R_v D_{\lambda v} = D_{\lambda v} D_{0v}$ . As follows from simplification, such filter must bring small error in the steady state mode only. The results obtained by the filter (13) are denoted in the Figures as the 1<sup>st</sup> estimate.

### QUASI-OPTIMAL KALMAN FILTER

If we take that  $\beta_v = 1$ ,  $H_v = 1$ , and  $u_v = 0$ , then we come to the following solution

$$\hat{\lambda}_v = \hat{\lambda}_{v-1} + k_v (\xi_v - \hat{\lambda}_{v-1}), \quad (14)$$

$$\frac{1}{R_v} = \frac{1}{R_{v-1} + D_{\lambda v}} + \frac{1}{D_{0v}}, \quad (15)$$

$$k_v = \frac{R_v}{D_{0v}}. \quad (16)$$

If  $D_{\lambda v} = D_\lambda$  and  $D_{0v} = D_0$  in (14)–(16) are the constant magnitudes, then the quasi-optimal Kalman filter appears. Here we may take the following assumptions. Let  $D_{\lambda v} = D_{\lambda 0}$  and  $D_{0v} = D_{00}$  be equal to the values known initially. For this case, we obtain the function marked in the Figures as the 2<sup>nd</sup> estimate. We also may evaluate the variances  $D_{\lambda v} = D_\lambda$  and  $D_{0v} = D_0$ , based on the regression line and obtain Kalman estimate starting from the certain discrete point. In Figure 1, we denoted this case the 3<sup>rd</sup> estimate.

### OPTIMAL KALMAN FILTER

Optimal estimates are obtained by (14)–(16) if all the necessary parameters of the observation and frequency behavior are known for the arbitrary time point. We get such values (strictly speaking, it is also quasi-optimal ones) based on the regression line

$$y_i = \bar{\xi} + \frac{\sigma_\xi}{\sigma_{t_i}} \rho_{\xi t_i} (t_i - \bar{t}), \quad i = \overline{0, m} \quad (17)$$

where  $\bar{\xi} = E\{\xi_i\}$  and  $\bar{t} = E\{t_i\}$  are expectations of  $\xi_i$  and  $t_i$  respectively,  $\sigma_\xi^2 = E\{(\xi_i - \bar{\xi})^2\}$  and  $\sigma_{t_i}^2 = E\{(t_i - \bar{t})^2\}$  are the corresponding variances,  $\rho_{\xi t_i} = \frac{E\{(\xi_i - \bar{\xi})(t_i - \bar{t})\}}{\sigma_\xi \sigma_{t_i}}$  is the correlation coefficient.

Procedure (17) takes first  $m$  points of the process for definition of the filter parameters by the following way. We put down  $\lambda(0) \equiv \lambda_{v-1} = y_m$ ; then we find out  $d\xi_v = \xi_v - y_v$  and obtain the values  $D_{0v} = E\{d\xi_v^2\}$ , (18). We further take the variance of the regression function (17) as  $\sigma_y^2 = M\{(y_i - \bar{y})^2\}$  and get  $D_{\lambda v} = D_{\lambda os} + \sigma_y^2$ , (19), where  $D_{\lambda os}$  is expected variance of an oscillator frequency. Let us note that function  $D_{\lambda v}$  depends on the regression function slope that results in the filter dynamic properties (inertia and inaccuracy). Finally, we take the initial value  $R_{v-1} = D_{\lambda m}$ . The optimal estimates are denoted as the 4<sup>th</sup> ones in the Figures.

### EXPERIMENTAL RESULTS

Figures 1-3 show the observation  $\xi_v$  formed by the OCXO frequency averaged over the time interval  $\Delta = 100$  sec with the GPS timing signals. Here we also show the measured frequency function  $f_v$  obtained

with use of the rubidium standard. We take it to compare with the received Kalman estimates and to evaluate the expected filtering errors for different algorithms. To get generalization we use the same observation for the all Kalman filters, noting that many experimental data **have been** processed in reality. Both 1<sup>st</sup> and 2<sup>nd</sup> estimates are based on the same constant values  $D_{0v} = D_0 = 5 \cdot 10^{-19}$ ,  $D_{\lambda v} = D_\lambda = 10^{-22}$ , and start zero point  $\lambda_0 = 0$ . In opposite, 3<sup>rd</sup> estimate is started approximately after three hours of regression processing and based on the automatically defined values  $\lambda(0) \equiv \lambda_{v-1} = y_m$ ,  $D_{0v}$  (18), and  $D_{\lambda v}$  (19) obtained by the linear regression function (17). Another benefit of the regression function (17) usage jointly with the one-dimensional algorithm (14)—(16) is **the possibility of** optimal Kalman filter creation. The procedure is similar to the above—**considered** (17)—(19). The difference is following. Here we use the sliding regression estimates of  $D_{0v}$ ,  $D_{\lambda v}$ , and  $\lambda_v$  based on which estimates  $\hat{\lambda}_{v-1}$  are provided through the Kalman algorithm (14)—(16). Figure 3 shows the optimal function (4<sup>th</sup> estimate) jointly with the curve obtained by the quasi-optimal filter (5<sup>th</sup> estimate). The major difference between those two algorithms is following. In the 4<sup>th</sup> case we use the variance function  $D_{\lambda v} = \tilde{D}_\lambda + \tilde{D}_{\lambda v}$ , where  $\tilde{D}_\lambda$  is the **desired filtering effect**, and  $\tilde{D}_{\lambda v}$  is the **additional increment depending on the estimate function rate** so that  $\tilde{D}_{\lambda v} = (\hat{\lambda}_v - \hat{\lambda}_{v-1}) / \Delta$ . In the 5<sup>th</sup> case, only equality  $D_{\lambda v} = \tilde{D}_\lambda$  is substituted.

## TWO-DIMENSIONAL ESTIMATES

Let us address to the two-dimensional Kalman filter pursuing the aim to get jointly the estimate  $\hat{f}_v$  of frequency  $f_v$  and estimate  $\hat{\alpha}_v$  of its aging rate  $\alpha_v$ , and to obtain the prediction  $\tilde{f}_v$ . Based on (1)—(8) we write [9]

$$\xi_v = \mathbf{H}_v \lambda_v + n_{0v}, \quad (18)$$

$$\lambda_v = \mathbf{A}_{v-1} \lambda_{v-1} + \mathbf{n}_{\lambda v}, \quad (19)$$

where

$$\mathbf{H}_v = \begin{bmatrix} 1 & 0 \end{bmatrix}, \quad (20)$$

$$\lambda_v = \begin{bmatrix} f_v \\ \alpha_v \end{bmatrix}, \quad (21)$$

$$\mathbf{A}_v = \begin{bmatrix} 1 & \Delta \\ 0 & 1 \end{bmatrix}, \quad (22)$$

$n_{0v}$  is a white Gaussian noise with discrete-time covariance  $V_{0v} = D_{0v} = E\{n_{0v}^2\} = N_{0v}/2\Delta$  and  $\mathbf{n}_{\lambda v}$  is a vector white Gaussian noise with covariance matrix [8, 3]  $\Psi_{\lambda v} = \frac{N_{\alpha v}}{2} \Delta \begin{bmatrix} \Delta^2/3 & \Delta/2 \\ \Delta/2 & 1 \end{bmatrix}$ , where  $N_{0v}/2$  and

$N_{\alpha v}/2$  are two-side continuous spectral densities of the noises  $n_{0v}$  and  $n_{\alpha v}$ . Correspondent prediction is formed through estimates  $\hat{f}_v$  and  $\hat{\alpha}_v$  by  $\tilde{f}_{v+1} = \hat{f}_v + \Delta \hat{\alpha}_v$ . Figure 3 shows the predicted curve (6<sup>th</sup> estimate) jointly with 4<sup>th</sup> estimate, for comparison. Here we see that the error in transient of prediction is more appreciable in comparison with the one-dimensional optimal case. Nevertheless, both optimal estimates obtain rather similar errors for the stationary observation data through 20 hours. So, in principle, direct frequency estimate is sufficient for prediction; that is extremely important for the synchronization needs when the GPS timing signal is not available.

## THREE-DIMENSIONAL ESTIMATES

Here we address to the most accurate Kalman algorithm based on the oscillator timing model [10].

## MATHEMATICAL MODEL OF THE OSCILLATOR TIMING SIGNAL

In the ideal case the total phase  $\Phi_{id}(t)$  of an ideal timing signal is presented by

$$\Phi_{id}(t) = 2\pi\nu_{nom}t \quad (23)$$

where:  $\nu_{nom}$  is called nominal frequency. Correspondingly, total instantaneous phase model of actual timing signals  $\Phi(t)$  is modeled as:

$$\Phi(t) = \Phi_0 + 2\pi\nu_{nom}(1 + y_0)t + \pi D\nu_{nom}t^2 + \varphi(t) \quad (24)$$

where:  $\Phi_0$  is the initial phase offset,  $y_0$  is the fractional frequency offset from the nominal value  $\nu_{nom}$  (mainly due to finite frequency settability of the clock);  $D$  is the linear fractional frequency drift rate (basically representing oscillator aging effects);  $\varphi(t)$  is the random phase deviation component. Based on the definition of time error and the above model (24), the following model for time error  $x(t)$  results:

$$x(t) = x_0 + (y_0 - y_{0,ref})t + \frac{D - D_{ref}}{2}t^2 + \frac{\varphi(t) - \varphi_{ref}(t)}{2\pi\nu_{nom}} \quad (25)$$

Assuming that for the measurement of  $x(t)$  the independent clock configuration applies and that the reference clock is properly chosen (i.e. all its degradation sources  $y_{0,ref}$ ,  $D_{ref}$ , and  $\varphi_{ref}(t)$  are negligible as compared to those of the clock under test), the  $x(t)$  model reduces to:

$$x(t) = x_0 + y_0t + \frac{D}{2}t^2 + \frac{\varphi(t)}{2\pi\nu_{nom}} \quad (26)$$

When the synchronized clock configuration applies and all slave clocks involved in the distribution of timing (including the clock under test) are operating in locked mode,  $y_{0,ref} = y_0$  and  $D_{ref} = D$  can be assumed; the  $x(t)$  model then reduces to:

$$x(t) = x_0 + \frac{\varphi(t) - \varphi_{ref}(t)}{2\pi\nu_{nom}} \quad (27)$$

## THREE DIMENSIONAL KALMAN FILTER

Based on the oscillator timing model (26) and the corresponding Kalman filter, one may expect the best filtering effect if the model and the filter are matched. Let us consider this possibility in detail using the model (26) and the algorithm (5)–(8) to create the corresponding three-dimensional Kalman filter. Decomposing the time error function  $x_v$  into the series, we write

$$x_v = x_{v-1} + y_{v-1}\Delta + 0.5\alpha_{v-1}\Delta^2 + n_{xv}, \quad (28)$$

where  $y_v = y_{v-1} + \alpha_{v-1}\Delta + n_{yv}$  is a frequency, and  $\alpha_v = \alpha_{v-1} + n_{av}$  is a linear component of frequency aging. It allows us to write the equation of the filter state in a form of (2) where

$$\lambda_v = \begin{bmatrix} x_v \\ y_v \\ \alpha_v \end{bmatrix}, \quad A_v = \begin{bmatrix} 1 & \Delta & \Delta^2/2 \\ 0 & 1 & \Delta \\ 0 & 0 & 1 \end{bmatrix}, \quad n_{\lambda v} = \begin{bmatrix} n_{xv} \\ n_{yv} \\ n_{av} \end{bmatrix}. \quad (29)$$

One-dimensional observation equation (1) is defined as

$$\xi_v = [\xi_v], \quad H_v = [1 \quad 0 \quad 0], \quad n_{0v} = [n_{0v}]. \quad (30)$$

Correspondingly, the Kalman filter equations are defined by (5)–(8), where for independent and uncorrelated noises we get

$$V_v = E\{n_{0v}n_{0v}^T\} = D_{0v} = S_{0v} \frac{1}{\Delta} = \frac{N_{0v}}{2\Delta} = \sigma_{0v}^2, \quad (31)$$

$$\Psi_v = E\{n_{\lambda v} n_{\lambda v}^T\} = \begin{bmatrix} \Psi_{11v} & \Psi_{12v} & \Psi_{13v} \\ \Psi_{21v} & \Psi_{22v} & \Psi_{23v} \\ \Psi_{31v} & \Psi_{32v} & \Psi_{33v} \end{bmatrix}, \quad (32)$$

где  $\Psi_{11v} = S_{xv}\Delta + S_{yv}\Delta^3/3 + S_{\alpha v}\Delta^5/20$ ;  $\Psi_{21v} = \Psi_{12v} = S_{yv}\Delta^2/2 + S_{\alpha v}\Delta^4/8$ ;  $\Psi_{22v} = S_{yv}\Delta + S_{\alpha v}\Delta^3/3$ ;  $\Psi_{33v} = S_{\alpha v}\Delta$ ;  $\Psi_{31v} = \Psi_{13v} = S_{\alpha v}\Delta^3/6$ ;  $\Psi_{32v} = \Psi_{23v} = S_{\alpha v}\Delta^2/2$ ;  $S_{xv} = N_{xv}/2$ ,  $S_{yv} = N_{yv}/2$  and  $S_{\alpha v} = N_{\alpha v}/2$  are correspondent two-side spectral densities of the continuous noises depending on the time interval  $\Delta$  in a general case. If to account an aging noise, only then matrix (32) yields

$$\Psi_v = \frac{N_{\alpha v}}{2} \Delta \begin{bmatrix} \Delta^4/20 & \Delta^3/8 & \Delta^2/6 \\ \Delta^3/8 & \Delta^2/3 & \Delta/2 \\ \Delta^2/6 & \Delta/2 & 1 \end{bmatrix} \equiv \frac{N_{\alpha v}}{2} \Delta \begin{bmatrix} 0 & 0 & 0 \\ 0 & 0 & 0 \\ 0 & 0 & 1 \end{bmatrix}. \quad (33)$$

**Corresponding** prediction equations are obtained by the above-considered algorithm being based on the estimates of  $\tilde{x}_v$ ,  $\hat{y}_v$  and  $\hat{\alpha}_v$  as follows

$$\begin{aligned} \tilde{x}_{v+1} &= \hat{x}_v + \hat{y}_v \Delta + 0.5 \hat{\alpha}_v \Delta^2, \\ \tilde{y}_{v+1} &= \hat{y}_v + \hat{\alpha}_v \Delta, \\ \tilde{\alpha}_{v+1} &= \hat{\alpha}_v. \end{aligned} \quad (34)$$

The equations (34), at bottom, are the working ones for the holdover operation mode of the slaved oscillator when GPS signals are not available [11].

## EXPERIMENTAL RESULTS

The results are given below for the Kalman algorithm (28)–(34) use for the synchronization error estimation. We consider the OCXO phase (time error) measured for  $\Delta = 100$  sec based on the GPS timing signals of the Motorola ONCORE UT+ Receiver. Here digital sequence  $x_v$  (the oscillator phase reduced to the time interval error) is the initial time error data that is processed by three-dimensional Kalman filter (28)–(34). As a result, we get the estimates  $\hat{x}_v$ ,  $\hat{y}_v$ , and  $\hat{\alpha}_v$ . Frequency estimate  $\hat{y}_v$  is compared with its accurate magnitude obtained by direct measurement with the use of the reference time signal of 1 sec of the rubidium standard in the same time scale. Figure 5 shows the initial observation (time error)  $x_v$  jointly with its Kalman estimate  $\hat{x}_v$  and expected error calculated as the difference  $\varepsilon_v = x_v - \hat{x}_v$ . Flowing from the physical sense, spectral density of the fluctuation of the aging speed within the noise matrix (33) is taken as  $S_{\alpha 0} = 0.5 N_{\alpha 0} \Delta = 4 \cdot 10^{-22} \text{ Hz}^2$  for the process. With this, the expected root-mean-square time deviation (TDEV) and maximal time interval error (MTIE) are estimated as  $\sigma_\varepsilon = 282.7 \text{ ns}$  and  $\Delta x_{\max} = 39680 \text{ ns}$ . Thus, in principle we get the **possibility** to reduce the time error by digital PLL to  $\Delta x_{\max} / \sigma_\varepsilon \approx 140$  times. Figure 6 exhibits the measured function of the relative frequency behavior of the same OCXO jointly with the Kalman estimate. If we take the measured data as the reference data, then the difference function may be taken as the error function, where TDEV equals  $\sigma_{\varepsilon v} = 146 \cdot 10^{-12}$  for the considered case. Correspondingly, TDEVs of the measured and estimated curves are  $\sigma_{ym} = 325 \cdot 10^{-12}$  and  $\sigma_y = 286 \cdot 10^{-12}$ . Hence, **the expected frequency control effect yields**  $a_y = \sigma_y / \sigma_{\varepsilon v} = 1.96$  and  $a_{ym} = \sigma_{ym} / \sigma_{\varepsilon v} = 2.4$  with respect to the measured and estimated data correspondingly. Finally, Figure 7 shows estimates obtained for the frequency aging. Mean value of  $\alpha_v$  equals  $\bar{\alpha}_v = E\{\alpha_v\} = -2.7 \cdot 10^{-15} / \text{s}$  upon the observation interval. TDEV for  $\alpha_v$  is equal to  $\sigma_\alpha = 3.4 \cdot 10^{-14} / \text{c}$ , **and the ratio of the two statistical estimates is**  $\sigma_\alpha / \bar{\alpha}_v = 12.4$  that is due to the extremely small  $\text{SNR} \ll 1$ .

## CONCLUSION

We have considered several Kalman algorithms intended for the time error, frequency, and aging estimation of the slaved oscillator being based on the Motorola GPS Oncore UT+ Timing Receiver. General findings of the studies are following. The best results of the parameter estimation are obtained if the timing model of the oscillator is known and matched with the filter dimension. Thus, selection of the proper Kalman algorithm has to be done at the early stage of the filtering and control to get the best effect. In this regard, three-dimensional algorithm is the most efficient for the rubidium oscillator and brings less good results for the crystal one, as the function of the crystal oscillator frequency behavior in time has the complex nature and is less predictable.

It follows that the stationary one-dimensional filter obtains accurate estimate with rather great noise. The quasi-optimal one with unknown initial statistics shows big error at the beginning stage of the process. Approximately the same results give the optimal one- and two-dimensional filters. Therefore, one-dimensional filters seem to be preferable for the fast and relatively accurate estimate of the only parameter (frequency, for instance). Two-dimensional ones allow prediction of the frequency offset and, therefore, are more preferable for synchronization tasks. Three-dimensional Kalman filters exhibit small inertia (negligible dynamic error) and high accuracy jointly with prediction of the time error for the holdover operation mode. This filter is well matched with a time model of the rubidium standard, and increase of the filter dimension is required in the case of a crystal oscillator, as usual. The filter adaptation gives good results for one- and two-dimensional algorithms. Contrarily, high adaptation efficiency for three-dimensional filters take place in the case only when the time error function exhibits a step character. Let us mark that such a case is not the usual one for the rubidium oscillators.

## REFERENCES

- [1] D.W. Allan and J.A. Barnes, "Optimal Time and Frequency Transfer Using GPS Signals," in *Proc. of the IEEE 36<sup>th</sup> AFCS*, pp.378-387, 1982.
- [2] R.L. Filler and S.R. Stein, "Kalman Filter Analysis for Real Time Applications of Clocks and Oscillators," in *Proc. of 42<sup>nd</sup> AFCS*, pp.447-452, 1988.
- [3] S.R. Stein, "Kalman Filter Analysis of Precision Clocks with Real-Time Parameter Estimation," in *Proc. of 43<sup>rd</sup> AFCS*, pp.232-236, 1989.
- [4] W. Su and R.L. Filler, "Application of Kalman Filtering Techniques to the Precision Clock with Non-Constant Aging," in *Proc. of 46<sup>th</sup> IEEE IFCS*, pp.231-237, 1992.
- [5] W. Su and R.L. Filler, "A New Approach to Clock Modeling and Kalman Filter Time and Frequency Prediction," in *Proc. of 47<sup>th</sup> IEEE IFCS*, pp.331-334, 1993.
- [6] R.E. Kalman, "A New Approach to Linear Filtering and Prediction Problems," *Trans. of the ASME, Ser.D, Journal of Basic Engr.*, Vol.82, pp.35-45, 1960.
- [7] R.K. Mehra, "On the Identification of Variances and Adaptive Kalman Filtering," *IEEE Trans. on Automatic Control*, Vol.15, No.2, pp.175-184, 1970.
- [8] B. Ekstrand, "Analytical Steady State Solution for a Kalman Tracking Filter," *IEEE Trans. on Aerospace and Electronic Systems*, Vol.19, No.6, pp.815-819, 1983.
- [9] O.E.Rudnev, Yu.S.Shmaliy, *et al.* "Kalman filtering of a frequency instability based on Motorola Oncore UT GPS Timing signals," *Proc. of 13<sup>th</sup> EFTF and 1999 IEEE IFCS*, 1999.
- [10] G.810. Definitions and terminology for synchronization networks, ITU-T, Geneva, Aug 1996.
- [11] W. Su and R.L. Filler, "A New Approach to Clock Modeling and Kalman Filter Time and Frequency Prediction," in *Proc. of 47<sup>th</sup> IEEE IFCS*, pp.331-334, 1993.



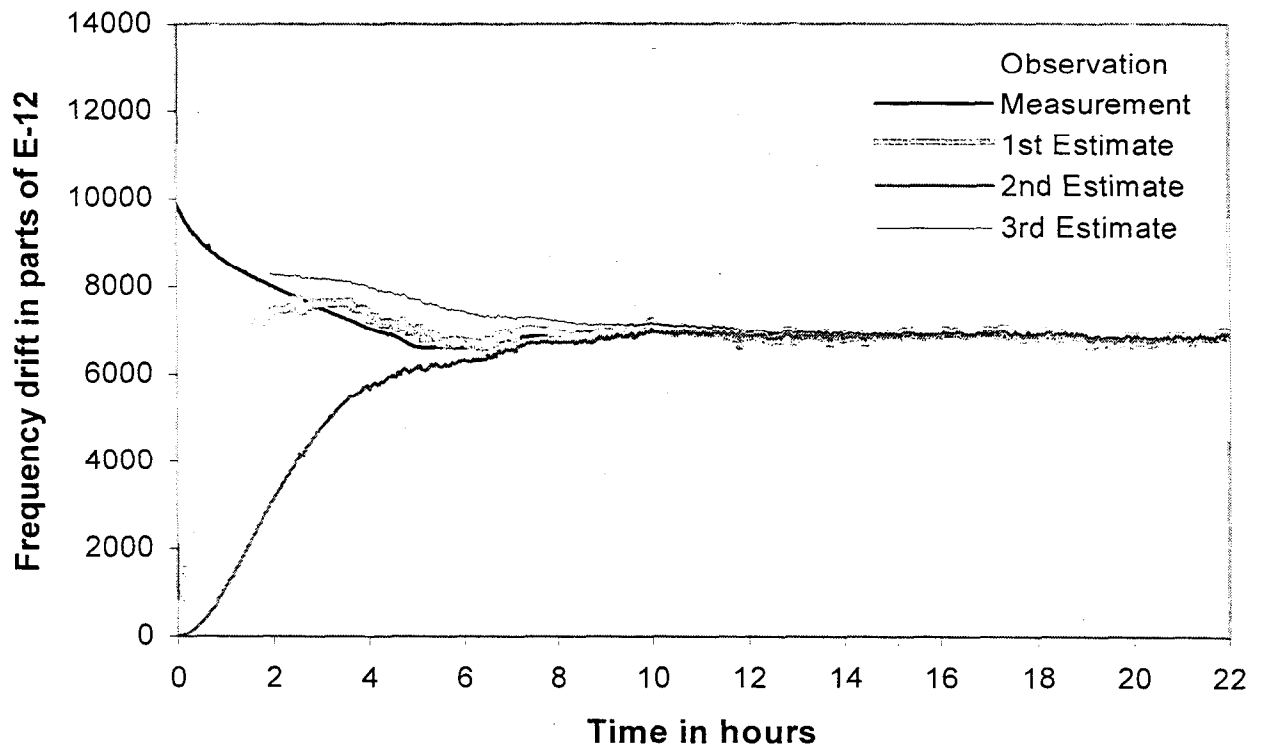


Figure 1. The Kalman estimates of the OCXO frequency, GPS-based observation, and measured data.

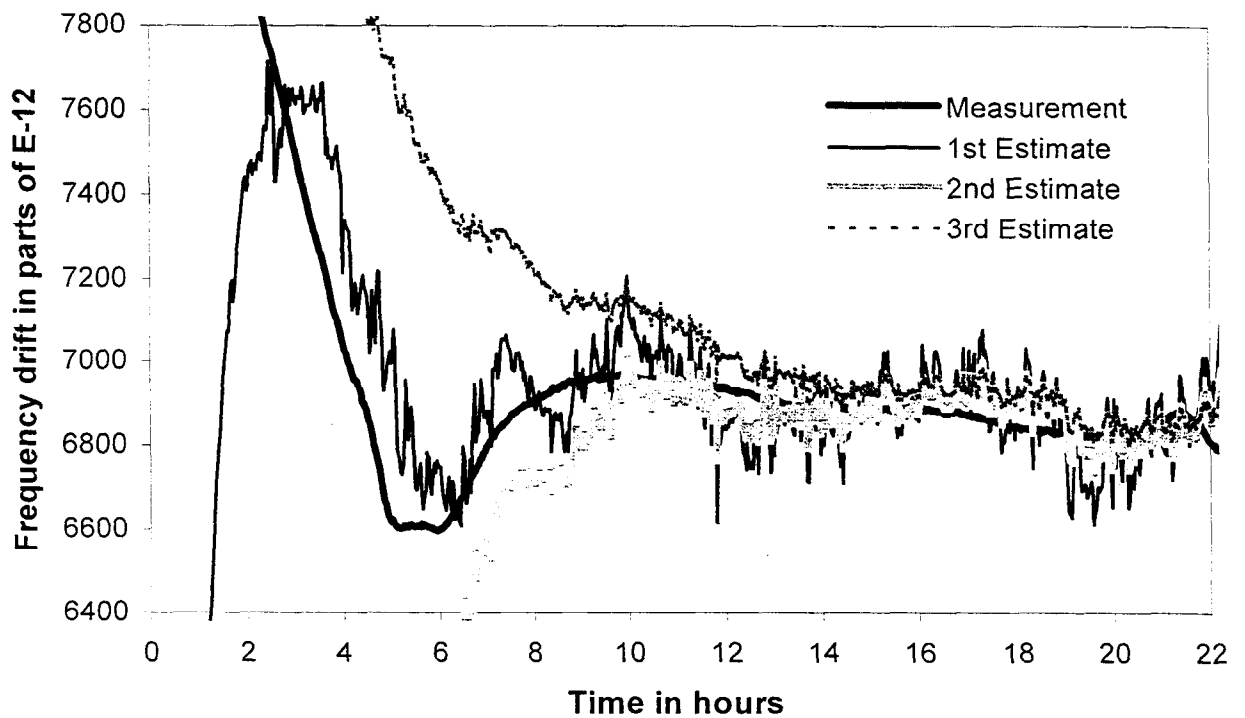


Figure 2. Magnified scales correspond to estimates obtained by the Figure 1.

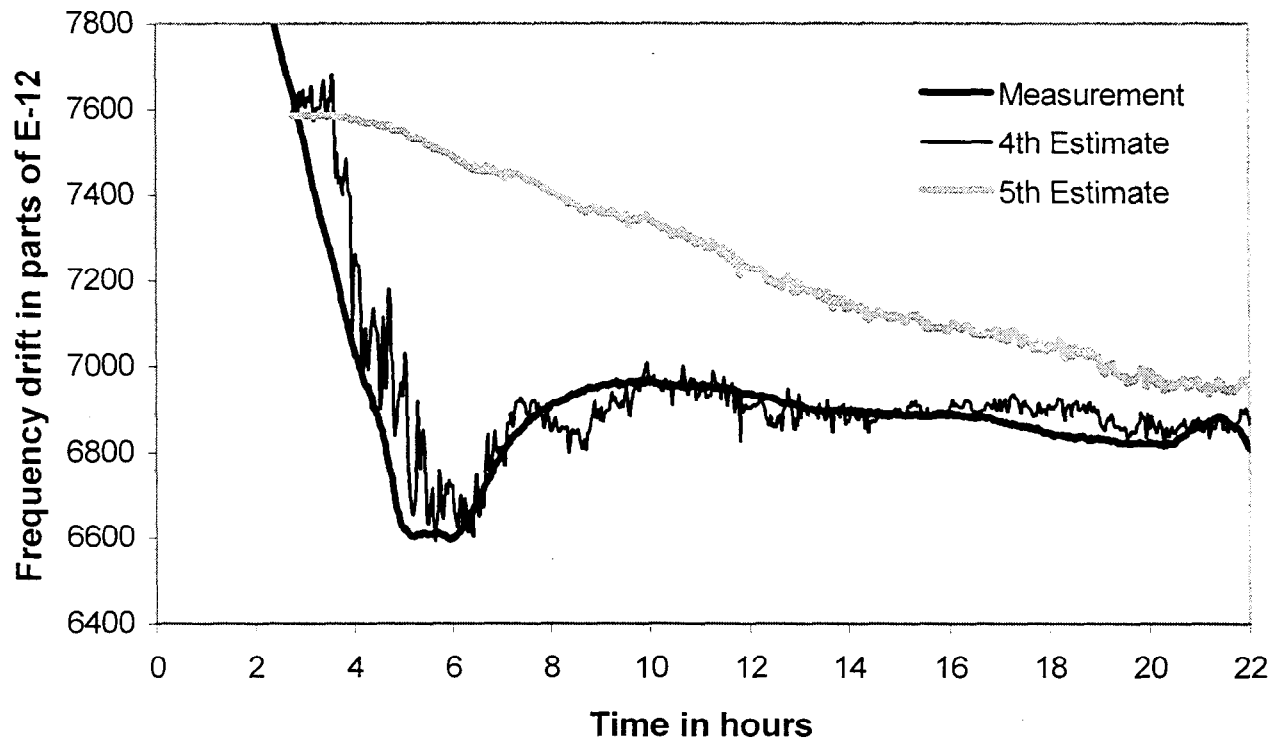


Figure 3. Magnified scales correspond to 4<sup>th</sup> and 5<sup>th</sup> estimates and measured data.

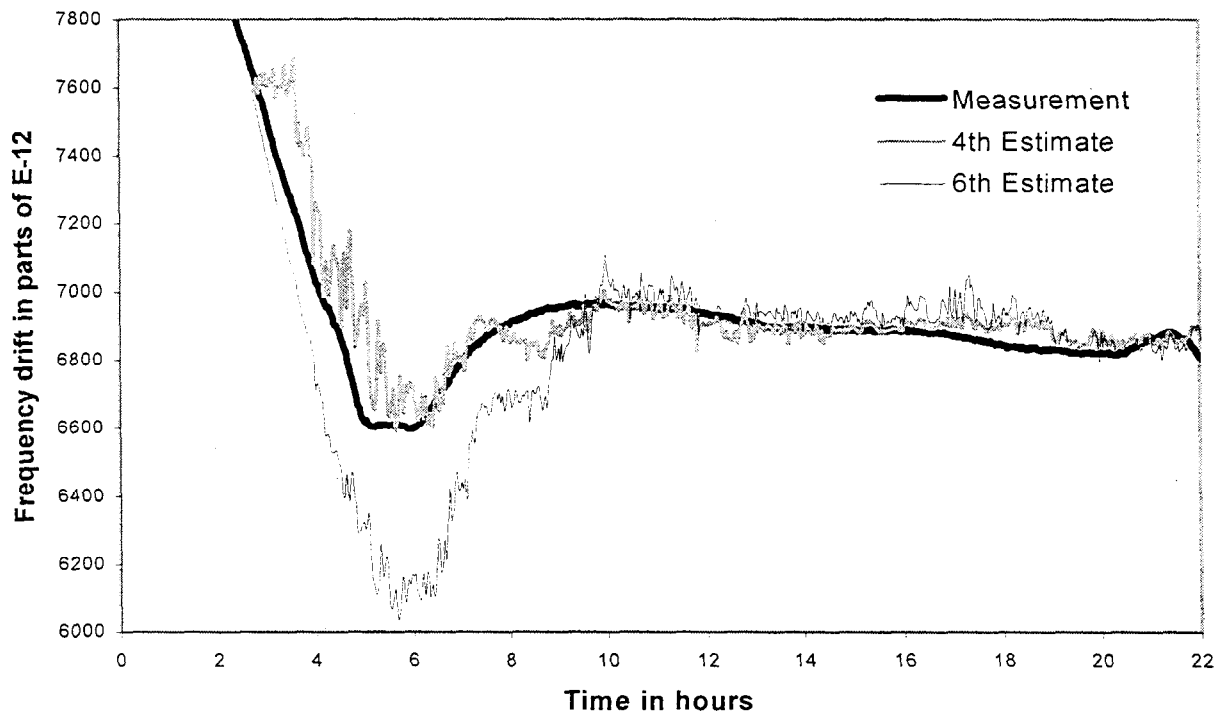


Figure 4. Magnified scales correspond to 4<sup>th</sup> one-state estimate and 6<sup>th</sup> two-state estimate (prediction).

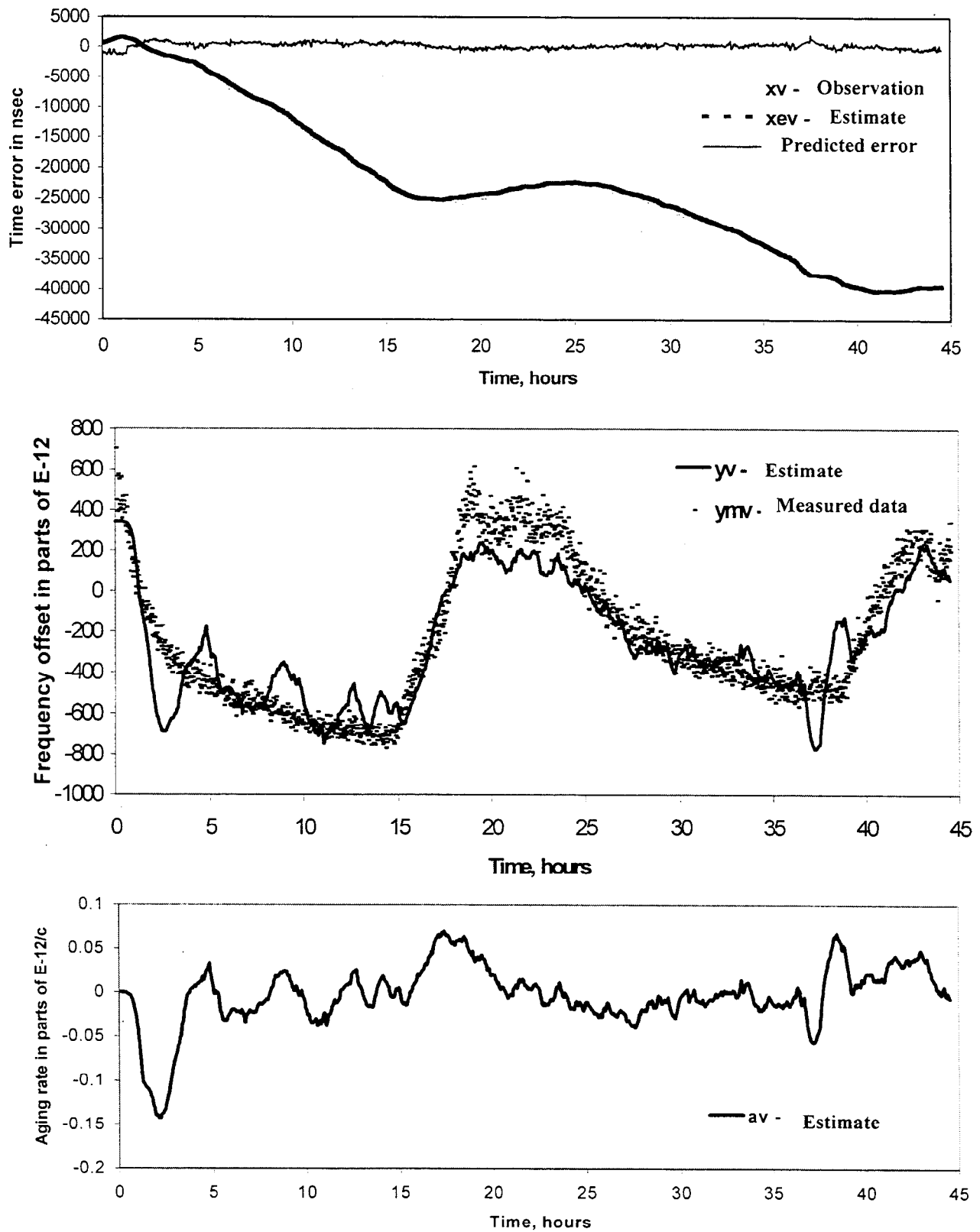


Figure 5. GPS-based three-state Kalman estimates of time error  $x_{ev} = \hat{x}_v$  (a), frequency offset  $y_v = \hat{y}_v$  and measured data (b), and frequency aging rate  $av = \hat{\alpha}_v$  (c).